Inorg. Chem. **2007**, *46*, 2805–2813

Optical and Redox Properties of Ruthenium Phthalocyanine Complexes Tuned with Axial Ligand Substituents

Tristan Rawling,[†] Hong Xiao,[†] Sang-Tae Lee,[‡] Stephen B. Colbran,[‡] and Andrew M. McDonagh*[,†]

Institute of Nanoscale Technology, University of Technology Sydney, Sydney, NSW 2007, Australia, and School of Chemistry, The University of New South Wales, Sydney, NSW 2052, Australia

Received September 28, 2006

The optical and electrochemical properties of the ruthenium phthalocyanine complexes [{(*t*-Bu)$_4$Pc}Ru(4-Rpy)$_2$], where R = NO_2, Me, NH_2, and NMe_2, are reported. The electron density at the macrocycle may be adjusted using the axial ligand substituents, which have varying electron-donating/withdrawing strengths. Electrochemical data show that the axial pyridine ligand substituents exert significant influence over the phthalocyanine ring-based redox processes. The axial ligands also influence the electronic absorption properties of the complexes with influence also being observed in the electrogenerated oxidized and reduced species.

Introduction

Metal phthalocyanine complexes have attracted sustained interest over many decades because of their interesting and useful optical and redox properties.[1−3] In addition to their traditional roles as dyes and pigments, the application of phthalocyanine complexes in areas such as photovoltaic devices,[4,5] catalysts,[6,7] gas sensors,[1,8,9] electrochromic displays,[10] and photodynamic therapy agents[11,12] has been investigated. Thus, the ability to tune the optical and electrochemical properties of phthalocyanine complexes is desirable, and several strategies have been employed to do this.

One approach is to include electron-withdrawing or -donating substituents on the periphery of the phthalocyanine ring, which has been shown to have a significant effect on electrochemical and optical properties.[13−15] Electron-donating groups increase electron density on the macrocycle, and redox processes occur at more negative potentials; the opposite effect occurs when electron-withdrawing groups are used. For example, the perfluorinated complex, [F_{16}PcRu] (where Pc = phthalocyanine), shows enhanced oxidative stability compared to that of [(PcRu)$_2$].[16,17]

Another approach involves axial ligand substitution of metal phthalocyanine complexes. A number of examples of six-coordinate transition metal phthalocyanine complexes have been reported, and the ability to vary the axial ligands provides a useful method to tune their properties.[18] In this study, ruthenium phthalocyanine complexes[19] with axial pyridine ligands were chosen because of their stability[20−22]

* To whom correspondence should be addressed. E-mail: Andrew.McDonagh@uts.edu.au.
[†] University of Technology Sydney.
[‡] The University of New South Wales.

(1) Leznoff, C. C., Lever, A. B. P., Eds. *Phthalocyanines: Properties and Applications*; VCH: New York, 1989.
(2) Thomas, A. L. *Phthalocyanine Research and Applications*; CRC Press: Boca Raton, FL, 1990.
(3) Armstrong, N. R. *J. Porphyrins Phthalocyanines* **2000**, *4*, 414.
(4) Yourre, T. A.; Rudaya, L. I.; Klimova, N. V.; Shamanin, V. V. *Semiconductors* **2003**, *37*, 807.
(5) Nazeeruddin, M. K.; Humphry-Baker, R.; Grätzel, M.; Murrer, B. A. *Chem. Commun.* **1998**, 719.
(6) Kaliya, O. L.; Lukyanets, E. A.; Vorozhtsov, G. N. *J. Porphyrins Phthalocyanines* **1999**, *3*, 592.
(7) d'Alessandro, N.; Liberatore, L.; Tonucci, L.; Morvillo, A.; Bressan, M. *J. Mol. Catal. A: Chem.* **2001**, *175*, 83.
(8) Generosi, A.; Albertini, V. R.; Rossi, G.; Pennesi, G.; Caminiti, R. *J. Phys. Chem. B* **2003**, *107*, 575.
(9) Guillaud, G.; Simon, J.; Germain, J. P. *Coord. Chem. Rev.* **1998**, *178−180*, 1433.
(10) Somani, P. R.; Radhakrishnan, S. *Mater. Chem. Phys.* **2003**, *77*, 117.
(11) Clarke, M. J. *Coord. Chem. Rev.* **2002**, *232*, 69.
(12) Tedesco, A. C.; Rotta, J. C. G.; Lunardi, C. N. *Curr. Org. Chem.* **2003**, *7*, 187.
(13) Yilmaz, I.; Guerek, A.; Ahsen, V. *Polyhedron* **2005**, *24*, 791.
(14) Louati, A.; El Meray, M.; Andre, J. J.; Simon, J.; Kadish, K. M.; Gross, M.; Giraudeau, A. *Inorg. Chem.* **1985**, *24*, 1175.
(15) Christendat, D.; David, M.-A.; Morin, S.; Lever, A. B. P.; Kadish, K. M.; Shao, J. *J. Porphyrins Phthalocyanines* **2005**, *9*, 626.
(16) Balkus, K. J., Jr.; Eissa, M.; Lavado, R. *Stud. Surf. Sci. Catal.* **1995**, *94*, 713.
(17) Balkus, K. J., Jr.; Eissa, M.; Levado, R. *J. Am. Chem. Soc.* **1995**, *117*, 10753.
(18) Alexiou, C.; Lever, A. B. P. *Coord. Chem. Rev.* **2001**, *216−217*, 45.
(19) Rawling, T.; McDonagh, A. *Coord. Chem. Rev.* [Online early access] DOI: 10.1016/j.ccr.2006.09.011. Published Online: Oct 5, 2006.
(20) Pomposo, F.; Carruthers, D.; Stynes, D. V. *Inorg. Chem.* **1982**, *21*, 4245.
(21) Doeff, M. M.; Sweigart, D. A. *Inorg. Chem.* **1981**, *20*, 1683.
(22) Cammidge, A. N.; Berber, G.; Chambrier, I.; Hough, P. W.; Cook, M. J. *Tetrahedron* **2005**, *61*, 4067.

10.1021/ic061866u CCC: $37.00
Published on Web 03/02/2007

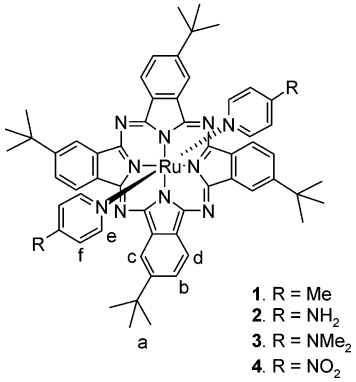

Figure 1. Complexes [{(*t*-Bu)$_4$Pc}Ru(4-Rpy)$_2$] investigated in this work.

and the interesting property that the phthalocyanine ring, rather than the metal center, undergoes redox processes at potentials generally accessible by cyclic voltammetry.[23] These complexes, therefore, allow for the effect of the axial ligand to be probed upon both oxidation and reduction of the phthalocyanine ring. Pyridine ligands with various 4-substituents were chosen, see Figure 1, to obtain a systematically varied series of complexes with different ligand electron-donor/acceptor strengths but without significant alteration to the metal−ligand bonding interaction. Even though these substituents are relatively remote from the phthalocyanine ring, we anticipated that they would exert some influence upon the optical and redox properties of the complexes. Importantly, the measurements reported here allow investigation of accessible oxidation and reduction processes while the metal center remains in the +2 oxidation state.

Axial ligands have been previously shown to affect the redox properties of metalloporphyrins, influencing redox potentials, as well as the sites of electron transfer.[24,25] In examples of ruthenium porphyrin complexes, the first oxidation is generally a reversible Ru$^{III/II}$ process.[24] However, coordination of an axial carbonyl ligand stabilizes the Ru^{II} oxidation state, and the first oxidation of this five-coordinate complex occurs at the porphyrin macrocycle.[26] The $E_{1/2}$ value of this oxidation process is influenced by coordination of various substituted pyridines at the remaining axial coordination site. Shifts of 100 mV were observed for a range of pyridine ligands bearing electron-withdrawing or -donating substituents.[27,28] The second oxidation of ruthenium porphyrin complexes has been reported to be an irreversible process and has been attributed to metal-centered oxidation, regardless of the axial ligands present.[24,28,29] The $E_{1/2}$ value is weakly influenced by the axial ligands.[26,28]

Few spectra of [Pc^{0}Ru^{II}] complexes have been reported;[23,30] a spectrum of [Pc^{0}Ru^{II}(CN)$_2$] has been presented, but considerable decomposition accompanied the formation this species.[30] No well-resolved spectra of [Pc^{0}Ru^{II}] examples have been forthcoming.

We present here the results of our investigations into the optical and electrochemical properties of the ruthenium phthalocyanine complexes, [{(*t*-Bu)$_4$Pc}Ru(4-Rpy)$_2$], where R = NO$_2$, Me, NH$_2$, and NMe$_2$ (Figure 1). We demonstrate that the electron density at the macrocycle may be adjusted using the axial ligand substituents, which have varying electron-donating/withdrawing strengths and report the first well-resolved spectra of the [{(*t*-Bu)$_4$Pc^0}Ru^{II}(4-Rpy)$_2$]$^{2+}$ dications.

Results and Discussion

Synthesis. Complexes **1**−**4** were prepared by modification of the synthetic method that Bossard et al.[31] used to prepare ruthenium phthalocyanine complexes with no peripheral substituents. In this study, complexes bearing peripheral *t*-butyl groups were prepared to improve their solubility.[32,33] Scheme 1 shows the synthetic procedure used in the current work. "Ruthenium blue", prepared by boiling RuCl$_3$·3H$_2$O in pentanol under a stream of dry nitrogen gas until the water was removed, was reacted with 4-*t*-butylphthalonitrile and hydroquinone under an ammonia atmosphere to give the tetra-*t*-butyl-substituted ruthenium phthalocyanine complex bearing two axial ammine ligands. We note that a mixture of four positional isomers is expected because of the arrangements of the *t*-butyl groups around the macrocycle.[34−36] No attempt was made to separate individual isomers. Unlike the analogous peripherally unsubstituted complex, [PcRu(NH$_3$)$_2$], which is insoluble in most solvents, the tetra-*tert*-butyl-substituted complex is soluble in many organic solvents. The reaction of the bisammine complex with benzonitrile gave [{(*t*-Bu)$_4$Pc}Ru(PhCN)$_2$] in good yield. Purification of [{(*t*-Bu)$_4$Pc}Ru(PhCN)$_2$] by column chromatography on silica or alumina gel significantly reduced yields so the crude product was used in subsequent reactions without further purification. The benzonitrile ligands were readily replaced with pyridine ligands under quite mild conditions. For example, the reaction of [{(*t*-Bu)$_4$Pc}Ru(PhCN)$_2$] with 4-substituted pyridines proceeded to completion within 3 h in refluxing dichloromethane. Purification by alumina column chromatography gave the desired products in moderate yields. The use of silica as a stationary phase for chromatography resulted in significantly lower isolated yields compared to neutral alumina. The complexes are

(23) Durr, K.; Hanack, M. *J. Porphyrins Phthalocyanines* **1999**, *3*, 224.
(24) Kadish, K. M.; Van Caemelbecke, E.; Royal, G. In *The Porphyrin Handbook*; Kadish, K. M., Smith, K. M., Guilard, R., Eds.; Academic Press: Burlington, VT, 2000; Vol. 8, p 1.
(25) Kadish, K. M.; Bottomley, L. A. *Inorg. Chem.* **1980**, *19*, 832.
(26) Brown, G. M.; Hopf, F. R.; Ferguson, J. A.; Meyer, T. J.; Whitten, D. G. *J. Am. Chem. Soc.* **1973**, *95*, 5939.
(27) Kadish, K. M.; Leggett, D. J.; Chang, D. *Inorg. Chem.* **1982**, *21*, 3618.
(28) Malerich, C. J. *Inorg. Chim. Acta* **1982**, *58*, 123.
(29) Li, Y.; Huang, J.-S.; Xu, G.-B.; Zhu, N.; Zhou, Z.-Y.; Che, C.-M.; Wong, K.-Y. *Chem.—Eur. J.* **2004**, *10*, 3486.
(30) Nyokong, T. *Polyhedron* **1993**, *12*, 375.
(31) Bossard, G. E.; Abrams, M. J.; Darkes, M. C.; Vollano, J. F.; Brooks, R. C. *Inorg. Chem.* **1995**, *34*, 1524.
(32) Hanack, M.; Hees, M.; Witke, E. *New J. Chem.* **1998**, *22*, 169.
(33) Dudnik, A. S.; Ivanov, A. V.; Tomilova, L. G.; Zefirov, N. S. *Russ. J. Coord. Chem.* **2004**, *30*, 110.
(34) Knecht, S.; Polley, R.; Hanack, M. *Appl. Organomet. Chem.* **1996**, *10*, 649.
(35) Sommerauer, M.; Rager, C.; Hanack, M. *J. Am. Chem. Soc.* **1996**, *118*, 10085.
(36) Weber, A.; Ertel, T. S.; Reinohl, U.; Feth, M.; Bertagnolli, H.; Leuze, M.; Hanack, M. *Eur. J. Inorg. Chem.* **2001**, 679.

Scheme 1. Syntheses of [{(*t*-Bu)$_4$*Pc*}Ru(4-Rpy)$_2$]

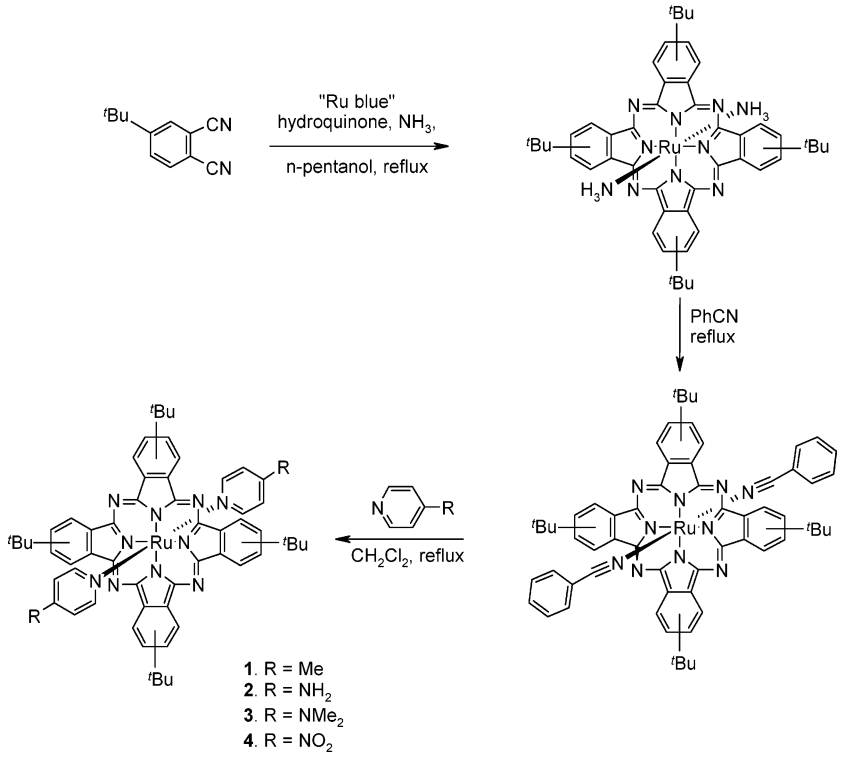

reasonably soluble in most organic solvents but are insoluble in water. Complex **1** has been prepared previously using a different synthetic procedure,[37] while **2**−**4** are new complexes.

^{1}H NMR Spectroscopy. The ^{1}H NMR spectra of **1**−**4** (see Table 1) are typical of [{(*t*-Bu)$_4$Pc}Ru(py)$_2$] complexes[37] but show variations that may be attributed to the different electron-withdrawing or -donating strengths of the pyridine substituents. The chemical shifts of the signals assigned to the *t*-butyl groups, a (see Figure 1), are virtually invariant across the series indicating little effect on these groups by the change in axial ligand substituent. In contrast, the signals assigned to the macrocyclic ring protons, b, shift downfield by 0.15 ppm upon moving from electron-donating NMe_2 or NH_2 groups to electron-withdrawing NO_2 4-substituents on the axial pyridines. Similar shifts are seen in the macrocyclic proton resonances c and d. The downfield shift for the macrocyclic protons indicates that the electron density of the phthalocyanine ring slightly decreases upon moving from electron-donating to electron-withdrawing substituents. The chemical shifts of the axial ligand protons are significantly upfield compared to those of the free ligand. For example, the ^{1}H NMR spectrum of 4-methylpyridine contains two doublets assigned to the ring protons at δ 8.50 and 7.14, while in the spectrum of **1**, these resonances occur at δ 5.01 and 2.36 for f and e, respectively. This large shift may be attributed to significant shielding of these protons resulting from their proximity to the diamagnetic ring current of the macrocycle;[23,38,39] shifts of this magnitude are not observed in complexes of the type *trans*-[RuL$_2$(R-py)$_2$], where L are bidentate ligands such as dioxolene[40] and bis(diphenylphosphino)butane,[41] or in *trans*-[RuCl$_2$(R-py)$_4$].[42] As with the macrocyclic protons, the protons of the pyridine ligands are deshielded more by the electron-withdrawing NO_2 group than by the electron-donating groups.

Table 1. ^{1}H NMR Chemical Shifts for **1**−**4** in $CDCl_3$

	chemical shift, δ (ppm)			
proton[a]	**1**	**2**	**3**	**4**
a	1.73	1.71	1.72	1.75
b	7.93	7.88	7.88	8.03
c	9.04	8.98	9.00	9.13
d	9.17	9.11	9.13	9.26
e	2.36	2.13	2.23	2.59
f	5.01	4.33	4.36	5.95

[a] See Figure 1 for assignments.

Electrochemistry. The electrochemistry of **1**−**4** was investigated by cyclic voltammetry. Electrochemical data are gathered in Table 2, and representative cyclic voltammograms of **1**−**4** are shown in Figure 2.

The cyclic voltammograms of **1**−**4** display two one-electron oxidation processes attributed to successive one-electron oxidations of the phthalocyanine macrocycle, that is, the [Pc$^-$Ru^{II}]$^+$/[Pc^{2-}Ru^{II}] and the [Pc^{0}Ru^{II}]$^{2+}$/[Pc$^-$Ru^{II}]$^+$ couples.[23,30] Spectroelectrochemistry confirms these assignments (see below). For each of these processes, the plots of

(37) Hanack, M.; Vermehren, P. *Chem. Ber.* **1991**, *124*, 1733.
(38) Bulatov, A.; Knecht, S.; Subramanian, L. R.; Hanack, M. *Chem. Ber.* **1993**, *126*, 2565.
(39) Gorbunova, Y. G.; Enakieva, Y. Y.; Sakharov, S. G.; Tsivadze, A. Y. *J. Porphyrins Phthalocyanines* **2003**, *7*, 795.
(40) Auburn, P. R.; Dodsworth, E. S.; Haga, M.; Liu, W.; Nevin, W. A.; Lever, A. B. P. *Inorg. Chem.* **1991**, *30*, 3502.
(41) Queiroz, S. L.; Batista, A. A.; Oliva, G.; Gambardella, M. T. d. P.; Santos, R. H. A.; MacFarlane, K. S.; Rettig, S. J.; James, B. R. *Inorg. Chim. Acta* **1998**, *267*, 209.
(42) Malecki, J. G.; Jaworska, M.; Kruszynski, R.; Gil-bortnowska, R. *Polyhedron* **2005**, *24*, 1445.

Table 2. Electrochemical Data from Cyclic Voltammetry Experiments[a]

	$E_{1/2}$, V vs Fc^+/Fc (ΔE_p, V)[b]			
process	**1**	**2**	**3**	**4**
Pc^{2-}, Pc^{1-}	0.07 (0.07)	−0.02 (0.06)	−0.02 (0.07)	0.22 (0.07)
Pc^{1-}, Pc^{0}	0.76 (0.08)	0.53 (0.07)	0.54 (0.07)	0.89 (0.11)
Pc^{2-}, Pc^{3-}	−1.90 (0.07)	−1.91 (0.07)	−1.93 (0.08)	−1.98 (0.10)
NO_2Py reduction				−1.14 (0.12)[c]
				−1.64[d]
other oxidation		1.17 (0.07)	1.13 (0.11)	

[a] In dichloromethane−$[Bu_4N][PF_6]$ (0.1 M) at a scan rate of 100 mV s^{-1}. [b] Reversible one-electron processes unless otherwise stated; ΔE_p (ferrocenium, ferrocene) = 65 mV. [c] Reversible two-electron process. [d] Cathodic peak for irreversible four-electron process.

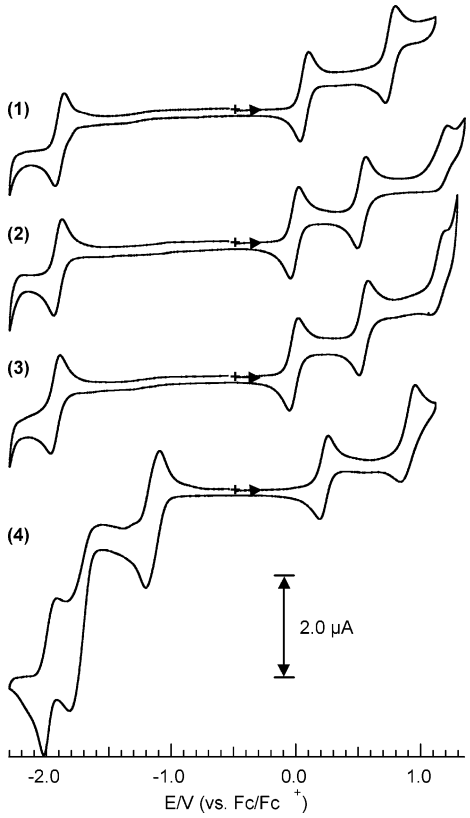

Figure 2. Cyclic voltammograms of **1**−**4** in dichloromethane solution with 0.1 M $[Bu_4N][PF_6]$ electrolyte. Scan rate = 100 mV s^{-1}.

i versus (scan rate)$^{1/2}$ are linear, which indicate diffusion-controlled Nernstian processes. The $E_{1/2}$ values reported for the two oxidations are similar to those reported for [{(*t*-Bu)$_4$Pc}Ru(3-Clpy)$_2$].[23] The potential data indicate that the substituents of the axial pyridine ligands exert considerable influence on the ring-based redox processes. The $[Pc^{-}Ru^{II}]^+$/$[Pc^{2-}Ru^{II}]$ couple for **2** and **3** is 90 mV more negative than that of **1**, while for **4**, it is 150 mV more positive. The $[Pc^{0}$-$Ru^{II}]^{2+}$/$[Pc^{-}Ru^{II}]^+$ couple follows the same trend. This is consistent with significant perturbation of the electron density of the macrocycle by the 4-substituents of the axial pyridine ligands, and the trend in oxidation potentials correlates with the pK_a values of the ligands[25,43] (Figure 3).

In the cyclic voltammograms of the amino-pyridine complexes, **2** and **3**, a third one-electron oxidation process

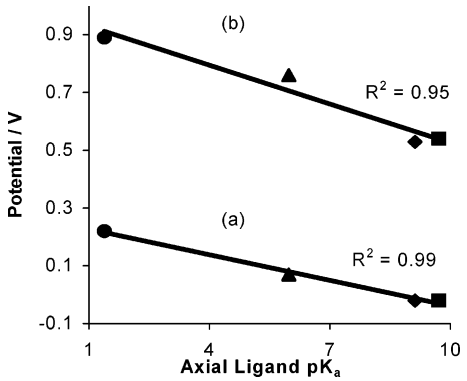

Figure 3. Graph showing oxidation potentials ($E_{1/2}$, V vs Fc^+/Fc) of **1**−**4** vs pK_a of the axial ligands, 4-Rpy (● = NO_2, ▲ = Me, ◆ = NH_2, ■ = NMe_2): (a) first oxidation and (b) second oxidation.

is observed near the onset of the anodic solvent discharge. This may be the Ru(III)/Ru(II) couple, lowered by the axial R_2N donor-substituted pyridines, or the reversible oxidation of one of these axial donors, in which case the R_2N-substituted pyridines must interact with each other (in an electrochemical sense) through the Ru center because the current clearly reveals a one-electron process. We are unable to distinguish between these alternatives at present.

The potentials for reduction of the macrocycle, which spectroelectrochemistry confirms is the $[Pc^{2-}Ru^{II}]$/$[Pc^{3-}$-$Ru^{II}]^-$ couple (see below), show significantly less variation across the series with a difference of only 80 mV between **1** and **4**. As expected, **2** and **3** have more negative reduction potentials than **1** because of their more electron-donating substituents. Interestingly, **4** has the most negative reduction potential for the $[Pc^{2-}Ru^{II}]$/$[Pc^{3-}Ru^{II}]^-$ couple in this series of complexes at −1.98 V (vs Fc^+/Fc). An examination of the redox behavior of nitro-aromatic compounds is helpful to see why this occurs.[44−46] Cyclic voltammograms of **4** reveal two additional reduction processes prior to the $[Pc^{2-}$-$Ru^{II}]$/$[Pc^{3-}Ru^{II}]^-$ couple. The first process is reversible and from peak currents is a two-electron process, while the second reduction is an irreversible multielectron process. These processes may be attributed to nitro group-centered reductions. The observation of a two-electron reversible couple suggests that concurrent one-electron reduction of each axial nitro-pyridine occurs to afford the corresponding nitro-pyridyl radical anion (eq 1). This assignment is consistent with the electrochemistry of nitrobenzene in aprotic solvents, which reveals a reversible one-electron reduction to give a stable anion radical.[44] Concurrent reduction processes imply that the axial ligands do not communicate with each other in an electrochemical sense through the $[Pc^{2-}Ru^{II}]$ core.

$$O_2NPy-(Pc^{2-})Ru^{II}-PyNO_2 + 2e^- \rightleftarrows O_2N^{\bullet-}Py-(Pc^{2-})Ru^{II}-PyNO_2^{\bullet-} \quad (1)$$

(43) Farrington, D. J.; Jones, J. G.; Robinson, N. D.; Twigg, M. V. *Transition Met. Chem.* **1999**, *24*, 697.
(44) Smith, W. H.; Bard, A. J. *J. Am. Chem. Soc.* **1975**, *97*, 5203.
(45) Nunez-Vergara, L. J.; Squella, J. A.; Olea-Azar, C.; Bollo, S.; Navarrete-Encina, P. A.; Sturm, J. C. *Electrochim. Acta* **2000**, *45*, 3555.
(46) Kokkinidis, G.; Papanastasiou, G. *Electrochim. Acta* **1989**, *34*, 803.

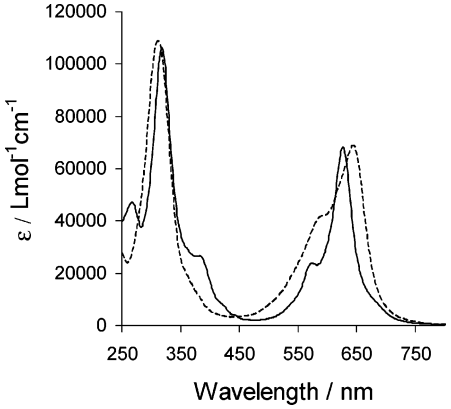

Figure 4. UV−vis spectra of **3** (solid line) and **4** (dashed line) in dichloromethane.

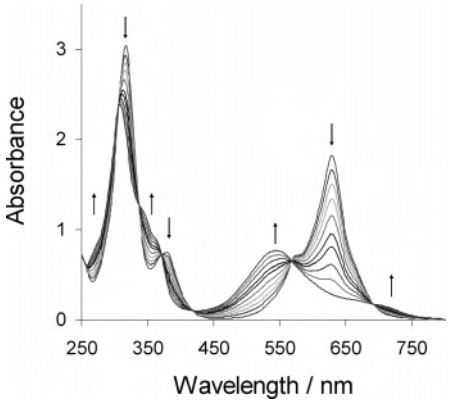

Figure 5. UV−vis spectra recorded during the first oxidation of **1** (at 0.39 V vs Fc^+/Fc) in dichloromethane/0.1 M [*n*-Bu_4N][PF_6]. Isosbestic points at 691, 568, 418, 371, 337, 306, and 254 nm.

On the basis of the reported reductive electrochemistry of the nitro-aromatics,[44,47,48] the subsequent process is tentatively assigned to concurrent reductions to afford axial hydroxylamine-substituted pyridine groups, although we cannot discount other alternatives. This second reduction process is irreversible because of its proton dependence (protons stripped from the solvent medium) and most probably proceeds with the loss of an oxygen from each nitro group as hydroxide or water.

Thus, the reduction potential for the $[Pc^{2-}Ru^{II}]/[Pc^{3-}Ru^{II}]^-$ couple of **4** occurs at a more negative potential than those of **1**−**3** because of the prior reductions involving the 4-nitro substituents of the axial ligands to give groups that behave as electron donors. This is also confirmed by spectroelectrochemical measurements (see below).

In summary, the electrochemical data show that the axial ligand substituents exert significant influence over the ring-based oxidation processes. The trends in the redox potentials are consistent with the trends in the electron-withdrawing or -donating strengths of the axial ligand substituents.

UV−Vis Spectroscopy. The UV−vis spectra of **3** and **4** are shown in Figure 4, and data for **1**−**4** are gathered in Table 3. The spectra of **1**−**3** are quite similar to each other with the characteristic Q-band observed at 626−627 nm and the Soret band at 317−318 nm. The Q-bands and Soret bands in **1**−**3** also have shoulders at 573−576 and 378−382 nm, respectively. In addition, the spectra of **2** and **3**, which both bear amine substituents on the axial ligands, display additional absorption bands at 243 nm in **2** and 267 nm in **3**.

In the spectrum of **4**, the Q-band maximum is observed at 645 nm, a bathochromic shift of ∼450 cm^{-1} compared to the other complexes, while the Soret band is seen at 312 nm, a hypsochromic shift of 600 cm^{-1}. The low-energy shoulder to the Soret band, observed at ∼380 nm in **1**−**3**, is also found in **4** at 382 nm; however, the intensity is greatly decreased.

Spectroelectrochemistry. To further probe the effect of the axial ligand substituents on optical and redox properties, UV−vis−NIR spectroelectrochemical experiments were performed on **1**−**4**. Spectroscopic data are shown in Table 3.

$[Pc^-Ru^{II}]^+/[Pc^{2-}Ru^{II}]$ Couple. Figure 5 shows the development of the UV−vis spectrum with time as the oxidation of **1** proceeds. For each of **1**−**4**, as the oxidation proceeds, the Q-band at ∼630 nm is replaced with a broad band at ∼540 nm with a pronounced low-energy tail. The Soret band blue shifts by 600−900 cm^{-1} and weakens slightly in intensity. The shoulder of the Soret band, observed in **1**−**3**, also disappears as the oxidation proceeds. The

Table 3. Electronic Absorption Maxima and Molar Absorptivities[a] of [{(*t*-Bu)$_4$Pc}Ru(4-Rpy)$_2$] Complexes

species	λ_{max}, nm [ϵ, M^{-1} cm^{-1}]
1 ([{(*t*-Bu)$_4$Pc^{2-}}Ru^{II}(4-Mepy)$_2$])	627 [68 000], 576sh, 378sh, 317 [110 000]
1$^+$ ([{(*t*-Bu)$_4$Pc$^-$}Ru^{II}(4-Mepy)$_2$]$^+$)	545 [29 000], 364sh, 344sh, 308 [89 000]
1^{2+} ([{(*t*-Bu)$_4$Pc^0}Ru^{II}(4-Mepy)$_2$]$^{2+}$)	441 [24 000], 310 [45 000], 276sh, 240 [46 000]
1$^-$ ([{(*t*-Bu)$_4$Pc^{3-}}Ru^{II}(4-Mepy)$_2^{\cdot-}$)	654sh, 632 [24 000], 551 [34 000], 352sh, 318 [48 000]
2 ([{(*t*-Bu)$_4$Pc^{2-}}Ru^{II}(4-NH$_2$py)$_2$])	627 [71 000], 573sh, 382sh, 318 [110 000], 243
2$^+$ ([{(*t*-Bu)$_4$Pc$^-$}Ru^{II}(4-NH$_2$py)$_2$]$^+$)	600sh, 560 [30 000], 366, 312 [88 000], 251
2^{2+} ([{(*t*-Bu)$_4$Pc^0}Ru^{II}(4-NH$_2$py)$_2$]$^{2+}$)	576 [37 000], 385, 307sh, 282 [62 000]
2$^-$ ([{(*t*-Bu)$_4$Pc^{3-}}Ru^{II}(4-NH$_2$py)$_2$]$^-$)	627 [23 000], 565 [13 000], 319 [39 000]
3 ([{(*t*-Bu)$_4$Pc^{2-}}Ru^{II}(4-NMe$_2$py)$_2$])	626 [66 000], 573sh, 382sh, 318 [105 000], 267
3$^+$ ([{(*t*-Bu)$_4$Pc$^-$}Ru^{II}(4-NMe$_2$py)$_2$]$^+$)	602 [29 000], 575sh, 366sh, 312 [74 000], 273sh
3^{2+} ([{(*t*-Bu)$_4$Pc^0}Ru^{II}(4-NMe$_2$py)$_2$]$^{2+}$)	576 [14 000], 383, 281 [66 000]
3$^-$ ([{(*t*-Bu)$_4$Pc^{3-}}Ru^{II}(4-NMe$_2$py)$_2$]$^-$)	627 [23 000], 556 [31 000], 318 [40 000]
4 ([{(*t*-Bu)$_4$Pc^{2-}}Ru^{II}(4-NO$_2$py)$_2$])	645 [69 000], 591sh, 382sh, 312 [109 000]
4$^+$ ([{(*t*-Bu)$_4$Pc$^-$}Ru^{II}(4-NO$_2$py)$_2$]$^+$)	555 [34 000], 323sh, 305 [84 000], 277sh
4^{2+} ([{(*t*-Bu)$_4$Pc^0}Ru^{II}(4-NO$_2$py)$_2$]$^{2+}$)	559sh, 407 [29 000], 295 [54 000], 278sh
4^{2-} ([{(*t*-Bu)$_4$Pc^{2-}}Ru^{II}(4-NO$_2^{\bullet-}$py)$_2$]$^{2-}$)	629 [85 000], 573sh, 391sh, 320 [94 000]
4^{3-} ([{(*t*-Bu)$_4$Pc^{3-}}Ru^{II}(4-NO$^{\bullet-}$py)$_2$]$^{3-}$)	630 [40 000], 570 [30 000], 321 [46 000]

[a] Calculated assuming 100% conversion of the parent complex.

(47) Morkovska, P.; Hromadova, M.; Pospisil, L.; Giannarelli, S. *Langmuir* **2006**, *22*, 1896.
(48) Silvester, D. S.; Wain, A. J.; Aldous, L.; Hardacre, C.; Compton, R. G. *J. Electroanal. Chem.* **2006**, *596*, 131.

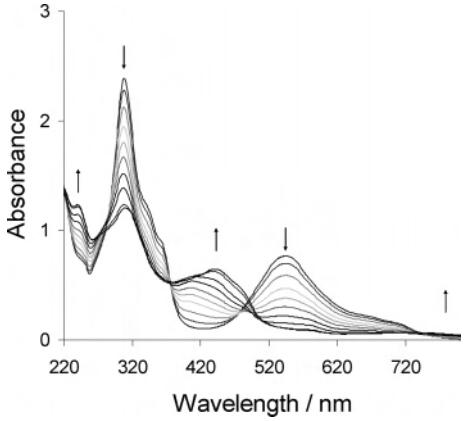

Figure 6. UV−vis spectra recorded during the second oxidation of **1** at up to +1.1 V vs Fc^+/Fc in dichloromethane (0.1 M [*n*-Bu_4N][PF_6]).

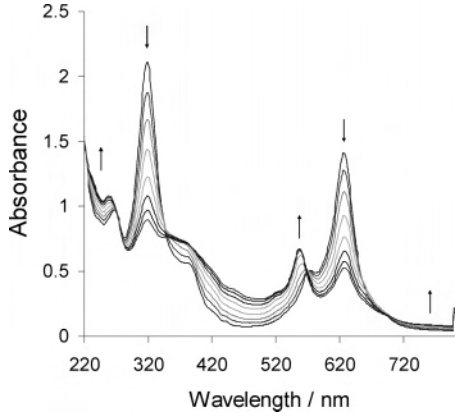

Figure 7. UV−vis spectra recorded during the first reduction of **3** at up to −2.2 V vs Fc^+/ Fc in dichloromethane (0.2 M [*n*-Bu_4N][PF_6]).

changes are characterized by distinct, clean isosbestic points and were fully reversed by re-reduction.

The UV−vis spectra for $\mathbf{1}^+$−$\mathbf{4}^+$ are consistent with the occurrence of a one-electron oxidation centered on the phthalocyanine ring, that is, the $[Pc^-Ru^{II}]^+/[Pc^{2-}Ru^{II}]$ couple. Because the Q-band is effectively a ring-centered HOMO to LUMO transition,[49] it is expected that it should be dramatically affected by oxidation of the macrocyclic ring. The Soret band, which contains contributions mainly from the HOMO−1 to LUMO transitions,[49] is expected to be only slightly perturbed by the oxidation. These spectra for $\mathbf{1}^+$−$\mathbf{4}^+$ are comparable to those previously reported for phthalocyanine π-cation radical metal complexes.[30,50−54] The changes in the spectra differ markedly from those of the reported ruthenium porphyrin complexes,[29] which is to be expected because the porphyrin examples involve metal-based processes.

In the UV−vis spectra of $\mathbf{3}^+$ and $\mathbf{4}^+$ (see Supporting Information), the Soret band of $\mathbf{4}^+$ is observed at ∼700 cm^{-1} higher energy than that of $\mathbf{3}^+$, similar to the trend in the parent species (see Figure 4). A comparison of the Q-band region reveals a different trend. In this region, $\mathbf{4}^+$ has a band at higher energy than those of $\mathbf{3}^+$, where (at least) two transitions are observed at 602 and 575 nm (shoulder). These data show that the axial ligand substituents continue to influence the optical properties of the complexes after oxidation of the macrocycle.

$[Pc^0Ru^{II}]^{2+}/[Pc^-Ru^{II}]^+$ Couple. Figure 6 shows the UV−vis spectra acquired as the oxidation of $\mathbf{1}^+$ proceeded. Upon oxidation of $\mathbf{1}^+$−$\mathbf{4}^+$ to the corresponding dications, $\mathbf{1}^{2+}$−$\mathbf{4}^{2+}$, each complex revealed slightly different behavior indicating that the 4-substituents on the axial pyridine ligands still have considerable influence over the spectra. As the oxidations of $\mathbf{1}^+$ and $\mathbf{4}^+$ proceed, the 540 nm band of the $[Pc^-Ru^{II}]^+$ π-cation radical disappears, and a new broad band at ∼450 nm appears. The Soret band weakens significantly, and a high-energy shoulder develops. During the oxidations of $\mathbf{2}^+$ and $\mathbf{3}^+$, the broad visible band at ∼560 nm was replaced by a sharper band at 576 nm. Weak but distinct bands at ∼750 and 384 nm also appear, and broadening, as opposed to a distinct band, is observed from 400−500 nm. Also, as these oxidations proceed, the Soret band of $\mathbf{2}^+$ broadens but that of $\mathbf{3}^+$ is replaced by a sharp, equally intense blue-shifted band at 290 nm. In all cases, clean isosbestic points were not observed, indicating that the processes are not fully reversible on the time scale of the experiment.

There are few examples of $[Pc^0Ru^{II}]$ complexes and their electronic spectra in the literature. Generation of the $[PcRu(py)_2]^{2+}$ dication by electrolysis was reported to be unachievable because of decomposition of the product.[50] Oxidation of $[PcRu(CN)_2]$ to the dication resulted in considerable decomposition, possibly because of oxidation of the axial cyanide ligands, and only a poorly resolved spectrum was recorded.[30] However, the disappearance of the Q band at ∼520 nm and the appearance of a band at ∼400 nm was observed, and the oxidation was tentatively assigned to a macrocycle-centered oxidation. Similar changes in electronic spectra were reported upon formation of $[Pc^0Os^{II}(L)_2]^{x+}$, where L = py or CN^- ligands.[55] The electronic spectrum of the species generated from oxidation of $[\{(neopentoxy)_4Pc^-\}Co^{III}]^{2+}$ is attributed to $[\{(neopentoxy)_4Pc^0\}Co^{III}]$ and shows bands centered at 430 and 630 nm.[56] Furthermore, the spectra observed[56] upon metal-centered oxidation of $[\{(neopentoxy)_4Pc^-\}Co^{II}]^+$ to $[\{(neopentoxy)_4Pc^-\}Co^{III}]^{2+}$ are quite different than those observed in this work. On the basis of these comparisons, we suggest that the well-resolved spectra of $\mathbf{1}^{2+}$−$\mathbf{4}^{2+}$ are indicative of a second ring-based oxidation, that is, the $[Pc^0Ru^{II}]/[Pc^-Ru^{II}]$ couple is observed rather than the $[Pc^-Ru^{III}]/[Pc^-Ru^{II}]$ couple.

(49) Stillman, M. J.; Nyokong, T. In *Phthalocyanines: Properties and Applications*; Leznoff, C. C., Lever, A. B. P., Eds.; VCH: New York, 1989; p 133.
(50) Dolphin, D.; James, B. R.; Murray, A. J.; Thornback, J. R. *Can. J. Chem* **1980**, *58*, 1125.
(51) Minor, P. C.; Gouterman, M.; Lever, A. B. P. *Inorg. Chem.* **1985**, *24*, 1894.
(52) Nyokong, T.; Gasyna, Z.; Stillman, M. J. *Inorg. Chem.* **1987**, *26*, 1087.
(53) Nyokong, T.; Gasyna, Z.; Stillman, M. J. *ACS Symp. Ser.* **1986**, *321*, 309.
(54) Nyokong, T.; Gasyna, Z.; Stillman, M. J. *Inorg. Chim. Acta* **1986**, *112*, 11.
(55) Sekota, M.; Nyokong, T. *Polyhedron* **1996**, *15*, 2901.
(56) Nevin, W. A.; Hempstead, M. R.; Liu, W.; Leznoff, C. C.; Lever, A. B. P. *Inorg. Chem.* **1987**, *26*, 570.

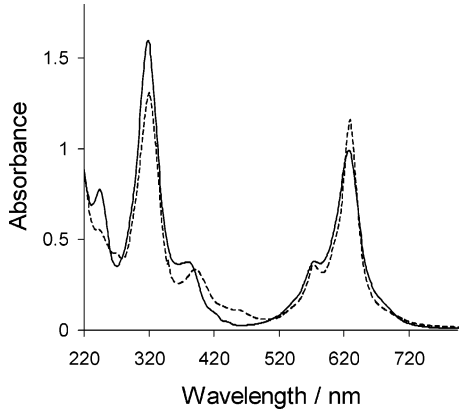

Figure 8. UV−vis spectra of **2** (solid line) and the electrochemically generated $\mathbf{4}^{2-}$ (dashed line) in dichloromethane.

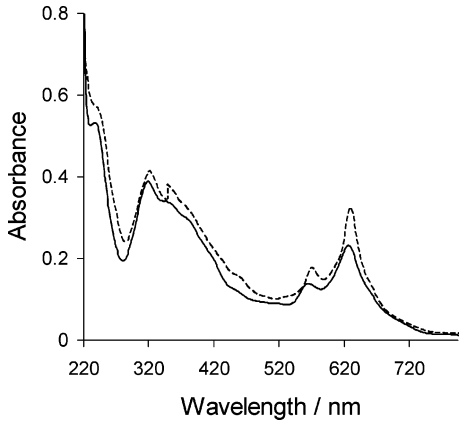

Figure 9. UV−vis spectra of $\mathbf{4}^{3-}$ (dashed line) and $\mathbf{2}^{-}$ (solid line) in dichloromethane.

$[Pc^{2-}Ru^{II}]/[Pc^{3-}Ru^{II}]^{-}$ Couple. Figure 7 illustrates the change in the UV−vis spectrum upon reduction of **3**. As the electrolyses proceeded, the Soret bands weakened and a pronounced low-energy structure appeared. The intensity of the Q-band greatly decreased as a second lower intensity Q-band at ∼560 nm appeared. The changes in these spectra are consistent with the macrocycle-centered reduction of **3** to $[Pc^{3-}Ru^{II}]^{-}$ ions.[15,51] Spectra obtained after the one-electron reduction of **1** and **2** are similar to that of $\mathbf{3}^{-}$, indicating **1** and **2** also undergo macrocycle-centered reduction. The absence of absolutely sharp isosbestic points again indicates some decomposition within the time scale of these experiments.

Reduction of 4. Cyclic voltammograms of **4** reveal that it has a more complicated reductive redox chemistry than **1**−**3** (see above). The reduction of **4** at a potential between those of the first and second reduction processes gives changes consistent with clean conversion from $[Pc^{2-}Ru^{II}(4\text{-}NO_2Py)_2]$ to $[Pc^{2-}Ru^{II}(4\text{-}NO_2^{\bullet-}Py)_2]^{2-}$. A comparison of the UV−vis spectrum of the generated anion with the spectrum of **2** is illustrative (see Figure 8). The spectra are remarkably similar, and the energies and shapes of the Q-band and the Soret band are virtually identical. A slight difference in the relative intensities of the bands is found with the Q-band and Soret band being of similar intensity in $\mathbf{4}^{2-}$, while the Q-band is more intense than the Soret band in **2**. We conclude that the electrogenerated nitro radical anion imparts electronic properties to the PcRu core similar to those imparted by the axial amino groups of **2**.

Because the irreversible multielectron reduction and the following reversible one-electron reduction processes for **4** are so close together (see the above discussion of the cyclic voltammetry), we were unable to separate them in the spectroelectrochemistry. Comparison of the electronic spectrum of the final reduction product with the electronic spectra of $\mathbf{1}^{-}-\mathbf{3}^{-}$, for example, Figure 9, clearly reveals that $[Pc^{3-}Ru^{II}]$ species forms. This is consistent with the anticipated production of the $[Pc^{3-}Ru^{II}(4\text{-}(HO)H_2N\text{-}py)_2]^{3-}$ species, an overall seven-electron reduction of $\mathbf{4}^{2-}$ (see above).

Conclusion

We have prepared and characterized four $[Pc^{2-}Ru^{II}(4\text{-}Rpy)_2]$ complexes, **1**−**4**, and the anions and cations that arise from their reduction or oxidation.

Electrochemical data show that the axial pyridine ligand substituents exert significant influence over the ring-based redox processes. The axial ligands also influence the electronic absorption properties of the complexes with the influence extending to all of the oxidized or reduced species studied. The electronic spectra of the $[Pc^{0}Ru^{II}(Rpy)_2]^{2+}$ dications, $\mathbf{1}^{2+}-\mathbf{4}^{2+}$, are the first well-resolved spectra reported for $[Pc^{0}Ru^{II}]^{2+}$ species.

This work demonstrates that adjustment of electron density at the phthalocyanine macrocycle can be achieved in six-coordinate complexes through the use of axial pyridine ligands with differing electron-withdrawing/accepting abilities. This control enables "fine-tuning" of the optical and electrochemical properties of phthalocyanine complexes.

Experimental Section

Physical Measurements. ^{1}H NMR spectra were recorded using a BVT 3000 Bruker Spectrospin instrument operating at 300.13 MHz. Spectra are referenced internally to residual protic solvent ($CHCl_3$, δ 7.26). See Figure 1 for the labels used in proton assignments. UV−vis spectra were recorded using a Agilent 8453 UV−vis spectrophotometer, in dichloromethane. Infrared spectra were recorded using a Nicolet Magna IR-760 spectrometer with complexes dispersed in KBr discs. Electrospray ionization mass spectra (ESI-MS) were recorded using a Perkin-Elmer SCIEX API300 triple quadrupole mass spectrometer. The general conditions were the following: ion spray voltage = 5000 V, drying gas temperature = 50 °C, orifice voltage = 30 V, ring voltage = 340 V, and injection via syringe pump. Spectra were averaged over 10 scans. Elemental microanalyses were carried out by the Microanalytical Service Unit at the Research School of Chemistry, Australian National University, Canberra, Australia. We note that the N analysis is consistently and significantly lower than the calculated values; a trend found in other reported microanalytical data for complexes of this type.[23,37,57]

(57) Hanack, M.; Osio-Barcina, J.; Witke, E.; Pohmer, J. *Synthesis* **1992**, 211.

Cyclic voltammetry measurements were performed in a conventional three-electrode cell using a computer-controlled Pine Instrument Co. AFCBP1 bipotentiostat as described in detail elsewhere.[58] The compounds were dissolved in dichloromethane (distilled over phosphorus pentoxide before use) with 0.1 M [*n*-Bu_4N][PF_6] as supporting electrolyte. The solutions were sparged with dry nitrogen gas before each measurement. Cyclic voltammograms were recorded with a 0.5 mm glassy carbon working electrode at scan rates ranging from 50 to 2000 mV s^{-1}. The potentials in this paper are quoted relative to the ferrocenium/ferrocene (Fe^{III}/Fe^{II}) couple measured under identical experimental conditions, which has a formal potential of 0.46 mV vs SCE[59] and occurred at 0.49 mV vs the Ag/AgCl/Cl^- (aq, 1 M) reference electrode employed in this work.

Solutions for spectroelectrochemistry experiments were prepared in a nitrogen-filled Braun glovebox operating with water and oxygen levels both below 2 ppm; the compounds were dissolved in anhydrous dichloromethane with [*n*-Bu_4N][PF_6] as supporting electrolyte. For all oxidations, a [*n*-Bu_4N][PF_6] concentration of 0.1 M was sufficient; however, a 0.2 M solution was required to explore all of the reductions. For reduction, the 0.2 M [*n*-Bu_4N]-[PF_6] concentration was used. The UV−vis−NIR spectroelectrochemical experiments were performed using a modified UV−vis−NIR cuvette with a Pt gauze working electrode, a Pt wire counter electrode, and an Ag/AgCl reference electrode in a Cary 5 spectrophotometer.

Chemicals. 4-*t*-Butylphthalonitrile was prepared by a modified literature procedure[60] from *t*-butylbenzene (Aldrich). 4-Nitropyridine was prepared by literature procedure.[61] The following were purchased commercially and used as received: $RuCl_3 \cdot 3H_2O$ (Precious Metals Online), *n*-pentanol (Aldrich), hydroquinone (Aldrich), benzonitrile (Aldrich), 4-methylpyridine (Aldrich), 4-aminopyridine (Koch-Light Laboratories), and 4-dimethylaminopyridine (Aldrich).

Syntheses. Preparation of [{(*t*-Bu)$_4$*Pc*}Ru(NH$_3$)$_2$]. The following procedure is an adaptation of the method of Bossard et al.[31] used to prepare [PcRu(NH_3)$_2$]. 4-*t*-Butylphthalonitrile (3.52 g, 19.1 mmol) and hydroquinone (0.2 g, 1.9 mmol) were dissolved in deoxygenated pentanol (20 mL). The mixture was refluxed under a stream of dry nitrogen gas. At the same time, $RuCl_3 \cdot 3H_2O$ (0.96 g, 3.7 mmol) was boiled in pentanol (10 mL) under a stream of nitrogen until a blue color formed. The $RuCl_3 \cdot 3H_2O$ was added over 5 min to the 4-*t*-butylphthalonitrile/hydroquinone mixture, and the resulting solution was refluxed under ammonia gas for 60 h. The reaction mixture was cooled, and the pentanol was removed by rotary evaporation. The blue solid was dissolved in dichloromethane:ethyl acetate (9:1) and passed through a plug of neutral alumina. After removal of the solvent by rotary evaporation, 2.60 g of a blue powder was collected. ^{1}H NMR (300 MHz, $CDCl_3$): δ 9.05 (m, 8H, H_d and H_c), 7.86 (m, 4H, H_b), 1.74 (m, 36H, H_a). MS: *m/z* 872 ([M + 2H]$^+$, 100).

Preparation of [{(*t*-Bu)$_4$Pc}Ru(PhCN)$_2$]. [(*t*-Bu_4Pc)Ru(NH_3)$_2$] (2.60 g, 2.99 mmol) was added to 25 mL of benzonitrile, and the mixture was heated at reflux for 24 h under a nitrogen atmosphere. After the mixture was cooled to room temperature, excess benzonitrile was removed in vacuo, affording 2.45 g of a crude product. ^{1}H NMR (300 MHz, $CDCl_3$): δ 9.35 (m, 4H, H_d), 9.22 (m, 4H, H_c), 8.03 (m, 4H, H_b), 6.82 (t, J_{HH} = 7.7 Hz, 2H, Ph), 6.49 (t, J_{HH} = 7.9 Hz, 4H, Ph), 5.52 (d, J_{HH} = 7.5 Hz, 4H, Ph) 1.76 (m, 36H, H_a). MS: *m/z* 1045 ([M + H]$^+$, 100).

Preparation of [{(*t*-Bu)$_4$Pc}Ru(4-Rpy)$_2$]. The same procedure was used to prepare each of the bispyridine complexes. The preparation of [{(*t*-Bu_4Pc}Ru(4-NO_2py)$_2$] is given as an example. 4-Nitropyridine (48 mg, 0.39 mmol) was added to a deoxygenated dichloromethane solution (20 mL) of crude [{(*t*-Bu_4Pc}Ru($PhCN)_2$] (135 mg, 0.13 mmol). The resulting solution was heated at reflux for 3 h under a nitrogen atmosphere. After the mixture was cooled to room temperature, the solvent was removed using a rotary evaporator. The crude product was purified by alumina column chromatography, eluting with dichloromethane/hexane (6:4), to yield 66 mg (47%) of a blue/purple powder. ^{1}H NMR (300 MHz, $CDCl_3$): δ 9.26 (m, 4H, H_d), 9.13 (m, 4H, H_c), 8.03 (m, 4H, H_b), 5.95 (d, J_{HH} = 7.2 Hz, 4H, H_f), 2.59 (d, J_{HH} = 6.9 Hz, 4H, H_e), 1.75 (m, 36H, H_a). IR (cm^{-1}): ν 2956 (s), 2900 (m), 2865 (m), 2361 (m), 1614 (w), 1590 (w), 1534 (s), 1489 (s), 1394 (m), 1363 (w), 1341 (vs), 1318 (w), 1280 (w), 1256 (m), 1191 (w), 1151 (s), 1126 (s), 1093 (m), 1051 (m), 1014 (w), 940 (w), 895 (w), 858 (m), 831 (m), 763 (m), 693 (m), 670 (m). UV−vis (λ_{max}, nm [ϵ, $\times 10^3$ M^{-1} cm^{-1}]): 645 [81], 591sh, 382sh, 312 [127]. MS: *m/z* 1088 ([M + 2H]$^+$, 100). Anal. Calcd for $C_{58}H_{56}N_{12}O_4$-Ru: C, 64.13; H, 5.20; N, 15.47. Found: C, 64.64; H, 5.64; N, 14.35.

[{(*t*-Bu)$_4$Pc}Ru(4-NH$_2$py)$_2$]. Yield: 30%, blue powder. ^{1}H NMR (300 MHz, $CDCl_3$): δ 9.11 (m, 4H, H_d), 8.98 (m, 4H, H_c), 7.88 (m, 4H, H_b), 4.33 (d, J_{HH} = 7.2 Hz, 4H, H_f), 3.07 (s, 4H, NH_2), 2.13 (d, J_{HH} = 6.9 Hz, 4H, H_e), 1.71 (m, 36H, H_a). IR (cm^{-1}): ν 3391 (m), 3216 (w), 3078 (w), 2957 (s), 2900 (m), 2866 (m), 2361 (m), 2340 (m), 1717 (m), 1699 (w), 1643 (s), 1576 (w), 1558 (m), 1540 (m), 1509 (s), 1492 (s), 1458 (m), 1395 (s), 1316 (m), 1280 (s), 1265 (s), 1214 (s), 1192 (w), 1153 (s), 1129 (m), 1093 (m), 1052 (s), 1023 (s), 942 (s), 827 (s), 765 (s), 693 (s), 668 (s). UV−vis (λ_{max}, nm [ϵ, $\times 10^3$ M^{-1} cm^{-1}]): 627 [71], 573sh, 382sh, 318 [110] 243. MS: *m/z* 1028 ([M + 2H]$^+$, 100). Anal. Calcd for $C_{58}H_{60}N_{12}$Ru: C, 67.88; H, 5.89; N, 16.38. Found: C, 66.80; H, 5.92; N, 14.65.

[{(*t*-Bu)$_4$Pc}Ru(4-NMe$_2$py)$_2$]. Yield: 47%, blue powder. ^{1}H NMR (300 MHz, $CDCl_3$): δ 9.13 (m, 4H, H_d), 9.00 (m, 4H, H_c), 7.88 (m, 4H, H_b), 4.36 (d, J_{HH} = 7.5 Hz, 4H, H_f), 2.23 (d, J_{HH} = 7.2 Hz, 4H, H_e), 2.00 (s, 12H, CH_3) 1.72 (m, 36H, H_a). IR (cm^{-1}): ν 3073 (w), 2957 (s), 2900 (w), 2865 (m), 2229 (w), 1718 (m), 1624 (s), 1530 (s), 1491 (s), 1444 (w), 1390 (s), 1363 (m), 1316 (s), 1280 (s), 1256 (s), 1229 (s), 1190 (m), 1152 (s), 1130 (m), 1092 (m), 1052 (s), 1021 (s), 942 (s), 894 (m), 829 (s), 808 (s), 762 (s), 694 (s), 668 (s), 535 (m). UV−vis (λ_{max}, nm [ϵ, $\times 10^3$ M^{-1} cm^{-1}]): 626 [66], 573sh, 382sh, 318 [105], 267. MS: *m/z* 1083 ([M + H]$^+$, 100). Anal. Calcd for $C_{62}H_{68}N_{12}$Ru: C, 68.80; H, 6.33; N, 15.53. Found: C, 68.69; H, 6.20; N, 13.60.

[{(*t*-Bu)$_4$Pc}Ru(4-Mepy)$_2$]. Yield: 33%, blue powder. ^{1}H NMR (300 MHz, $CDCl_3$): δ 9.17 (m, 4H, H_d), 9.04 (m, 4H, H_c), 7.93 (m, 4H, H_b), 5.01 (d, J_{HH} = 6.3 Hz, 4H, H_f), 2.36 (d, J_{HH} = 6.6 Hz, 4H, H_e), 1.73 (m, 36H, H_a), 1.14 (s, 6H, CH_3). IR (cm^{-1}): ν 3078 (w), 2957 (s), 2900 (m), 2864(m), 2361 (m), 2340 (w), 1717 (w), 1652 (w), 1617 (s), 1578 (w), 1558 (w), 1540 (w), 1492 (s), 1458 (w), 1394 (s), 1363 (s), 1316 (s), 1280 (s), 1256 (s), 1191 (s), 1152 (s), 1129 (m), 1092 (m), 1051 (s), 1023 (w), 941 (s), 894

(58) Sembiring, S. B.; Colbran, S. B.; Craig, D. C. *J. Chem. Soc., Dalton Trans.* **1999**, 1543.
(59) Connelly, N. G.; Geiger, W. E. *Chem. Rev.* **1996**, *96*, 877.
(60) Khanamiryan, A. K.; Bhardwaj, N.; Leznoff, C. C. *J. Porphyrins Phthalocyanines* **2000**, *4*, 484.
(61) Karramkam, M.; Hinnen, F.; Vaufrey, F.; Dolle, F. *J. Labelled Compd. Radiopharm.* **2003**, *46*, 979.

(s), 856 (m), 829 (s), 810 (m), 763 (s), 693 (s), 669 (s), 605 (m), 565 (w), 534 (m), 504 (m), 446 (m). UV−vis (λ_{max}, nm [ϵ, $\times 10^3$ M^{-1} cm^{-1}]): 627 [68], 576sh, 378sh, 317 [110]. MS: *m/z* 1026 ($[M + 2H]^+$, 100). Anal. Calcd for $C_{60}H_{62}N_{10}Ru$: C, 70.36; H, 6.10; N, 13.67. Found: C, 69.10; H, 6.05; N, 12.61. The ^1H NMR and UV−vis data reported here are in agreement with previously reported data.[37]

Acknowledgment. We thank Dr. Ronald Shimmon, UTS, for technical assistance, and the Australian Research Council for financial support. A.M.M. holds an ARC APD Fellowship.

Supporting Information Available: Spectroelectrochemical data. This material is available free of charge via the Internet at http://pubs.acs.org.

IC061866U